A Digital Time-lapse, Bright Field Technology to Drive Faster, Higher Throughput Label-free Bioanalysis

Chiara Canali,* Erik Spillum, Martin Valvik, Niels Agersnap, Tom Olesen

BioSense Solutions ApS, Hirsemarken 1, DK-3520 Farum, Denmark

The constant need to develop more rapid and cost-effective technologies for accurate, sensitive and specific detection in biological samples is a driving force behind the integration of new sample preparation tools, automation and informatics across the bioanalytical workflow. These technologies have potential applications in different fields of research ranging from microbiology, toxicology and medicinal chemistry to the pharmaceutical and cosmetic industries,[1] as well as food and environmental safety.[2] We present the design characteristics, operational features and key advantages of a new digital, time-lapse, bright field technology with demonstrated uses and great potential across a range of applications involving bioanalysis of microbial and mammalian cells.

For instance, the evaluation of the effect of active compounds that modulate a particular biochemical pathway in a specific microorganism can provide a starting point for drug design,[3] but it can also improve our understanding of the role of such a pathway in biology.[4] Higher throughput analysis facilitates simultaneous detection of the effect of multiple compounds in the same experiment and, hence, it can reduce the time, cost and labour associated with more conventional detection technologies. Higher throughput bioanalysis has been enabled by the integration of new sample handling tools used to prepare arrays of cells (e.g., microtiter plates), technologies for automated analysis (e.g., imaging systems) and informatics tools for large-scale data production, manipulation and storage, which have consequently boosted the development of so-called large-scale cell biology (LSCB).

In LSCB, several combinatorial experiments are performed in order to test multiple variables, such as cell type, drug concentration, treatment times, and different cellular parameters measured in the individual experiments at various frequencies and time points.[5] Such experiments make it possible to dissect biochemical pathways using highly relevant measurements made in intact cells and can play a significant role in the development of targeted antimicrobial agents[6] and "smart" chemotherapeutic drugs for personalised medicine.[7] Additionally, LSCB aims to gain insights into molecular details involved in multiple cellular activities that can be monitored in individual cells within a population in real time.[8] It is also an effective approach for screening the effects of suppression or amplification of gene expression to validate molecular targets and consequent therapeutic intervention.[9]

Existing Technologies: Challenges and Limitations

The integration of automated technologies for higher throughput bioanalysis, as well as data manipulation and management, are crucial for the development of LSCB in research and biotechnology. To date, light microscopy techniques have provided powerful tools for LSCB studies as they are compatible with living cells and allow high-sensitivity measurements of specific molecules and molecular events.[10] Automated microscopes and advances in digital image analysis have enabled higher throughput studies by automating the imaging process and overall cell-based analysis.[11] When selecting which optical technology to use for imaging living cells, three elements should be taken into account: sensitivity of detection, speed of acquisition and viability of the specimen. In this regard, light microscopy of living cells allows for acquisition of images with a high signal-to-noise ratio while reducing damage to the sample, which is a particularly critical issue in live cell imaging. Bright field microscopy is often used along with fluorescence microscopy to provide information on cell shape, position and motility.[12–14] Bright field microscopy, in which white light is transmitted through the sample, is the simplest available microscopy technique. The specimens absorb part of the transmitted light and, therefore, they appear darker compared to the background.[15,16]

Bright field microscopy is typically used in systems where the field of view (FoV) is relatively small. A small FoV limits the volume that can be imaged, thus introducing poor counting statistics for the objects being visualised in the sample. Moreover, in conventional bright field microscopy it is difficult to visualise so-called “phase objects,” for which light propagation through them results in a small phase shift of the light wave, which makes the object appear transparent. This

occurs with bacteria, some cell components in protozoans and several mammalian cells at the level of the cell nucleus, cytoplasm, organelles and even sperm tails. To overcome such challenges, phase contrast microscopy and confocal microscopy play an important role in biological imaging, providing increased optical resolution.[17] Phase contrast microscopy[18] converts phase shifts in light passing through the sample to brightness changes in the image, whereas confocal microscopy[19] only allows detection of the light produced by fluorescence very close to the focal plane. Such techniques provide increased optical resolution; however, they are expensive and require a long acquisition time and improper settings can cause significant artefacts in the images.[20]

New Digital, Time-Lapse Technology

To circumvent the limitations described above, we designed, developed and tested a new portable bright field technology for digital[21] time-lapse[22] scanning through a miniaturised sample. This technology is well suited for liquid samples such as bacterial cultures and clinical isolates (e.g., urine[23]) but also for solid cultures of a single bacterial colony growing on a semi-transparent medium. The method relies on an imaging system that consists of a digital camera, an illumination unit and a lens where the optical axis is tilted 6.25° relative to the horizontal plane of the stage (Figure 1). Due to this tilt, scanning of volumes and extraction of phase information are possible when recording a series of images along the scan direction to form an image stack. Therefore, the tilting of the optical axis grants also more freedom of operation at both high and low cell concentrations. When all the biological species (e.g., bacteria in Figure 1) are sedimented at the bottom of the sample container, an image stack is obtained, which is a parallelepiped covering the detection volume in the sample ($V_{detection}$) and contains the all-in-focus image as well as the adjacent out-of-focus images along the vertical axis.

$$V_{detection} = L \cdot H \cdot W \cdot \sin(6.25) \cdot n \qquad \text{(Equation 1)}$$

In Equation 1, L and H are the camera chip dimensions divided by the magnification factor, W is the scan length and n is the refractive index of the sample medium. Along the scan direction, the total number of longitudinal steps for image acquisition (N) can be chosen to cover up to the entire length of the sample, with a minimum step length of 7.5 µm. For instance, if an image stack consisting of two images separated by six steps is used, the perpendicular displacement between the object planes of the images (ΔZ_{plane}) in air and the detected volume ($V_{detection}$) will be:

$$\Delta Z_{plane} = \sin(6.25) \cdot 6 \cdot 7.5\ \mu m = 4.9\ \mu m \qquad \text{(Equation 2)}$$

$$V_{detection} = 4.9\ \mu m \cdot (N - 1) \cdot L \cdot n \qquad \text{(Equation 3)}$$

with L = 1.4 mm, H = 1.0 mm, W = 7.5 mm, and n = 1.34 for a water-like medium.[23]

An optical resolution of 1.3 µm is achieved using the proprietary lens system and a 5 Mpx complementary metal oxide semiconductor (CMOS) camera chip (5.6 mm length and 4.0 mm height) with a focus depth of ~ 10 µm and an optical magnification factor of 4. When all the biological species (Fig. 1) are sedimented at the bottom of the sample container, all objects of interest are caught in focus along the horizontal plane. The generated digital image can be visualised on a computer screen and recorded using a dedicated software (UniExplorer, BioSense Solutions ApS). Such technology is integrated in the oCelloScope imaging system (Fig. 2), with dimensions of 45 × 26 × 25 cm, which allows portability and the possibility of operation in standard laboratory incubators for biological applications (temperature: 20–40°C, humidity: 20–93%). The system has reduced scanning time down to 2 min 36 sec for a 96-well microtiter plate and supports different types of samples and containers including microscope slides and any kind of microtiter plate up to 96 wells.

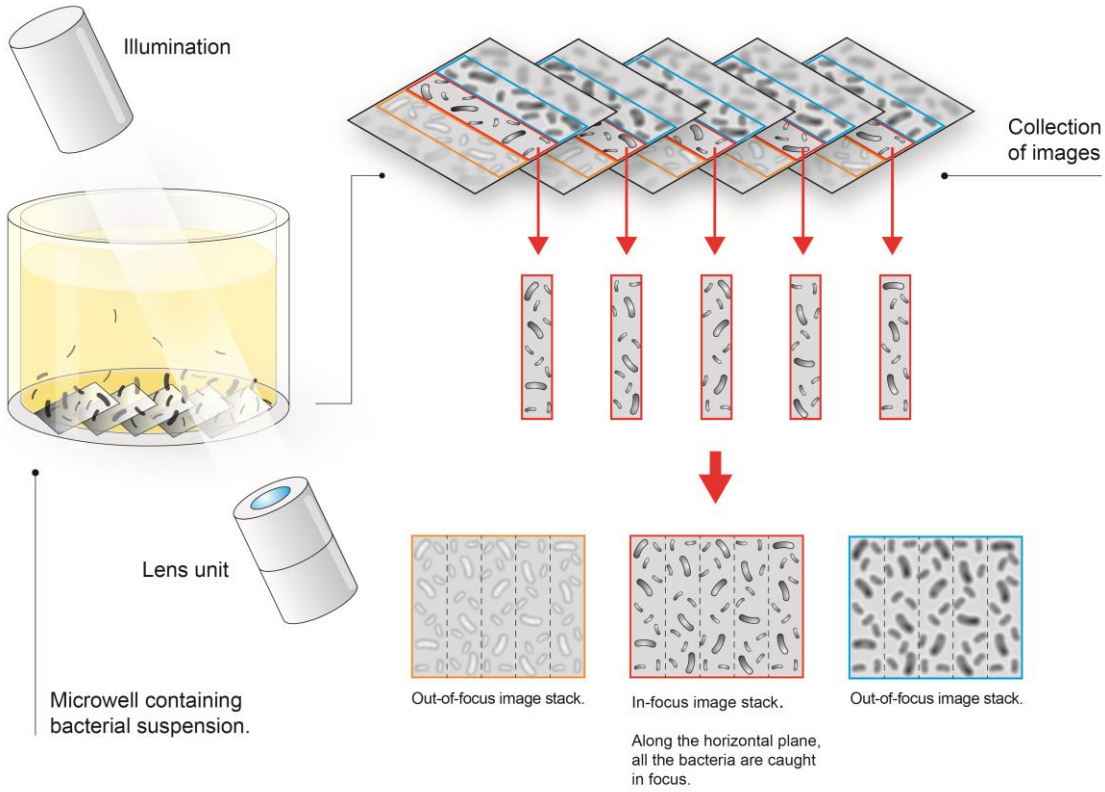

Figure 1. Schematic showing the oCelloScope optical scanning technology applied to a microwell containing a bacterial suspension. The optical axis of the miniaturised imaging system is tilted 6.25° relative to the horizontal plane of the stage to allow scanning of volumes. Images are acquired to form an image stack which contains the all-in-focus image as well as the adjacent out-of-focus images located along the vertical axis. As all the bacteria are sedimented at the bottom of the microwell, along the horizontal plane, all the bacteria are in focus.

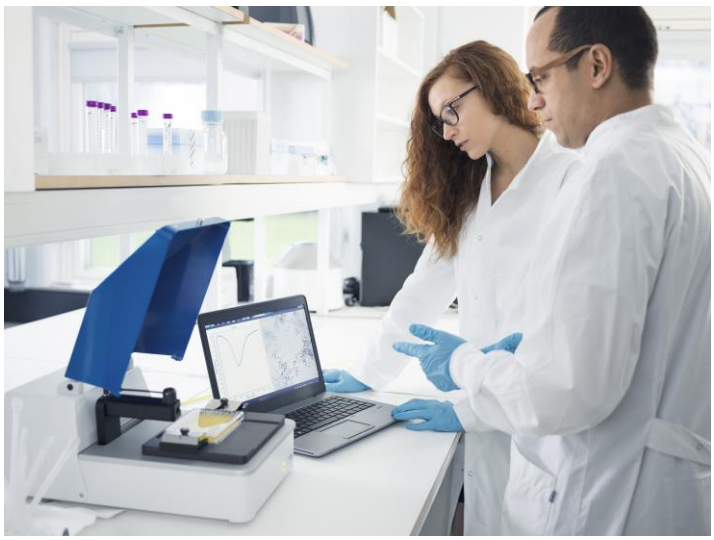

Figure 2. Photograph of the open oCelloScope imaging system loaded with a 96-well plate. The dedicated software displays images and curves resulting from a growth experiment performed on samples of *Saccharomyces cerevisiae*.

When setting an experiment, the focus and illumination level for image acquisition can be automatically adjusted through dedicated algorithms. Additional algorithms facilitate online image processing and analysis. These include (i) estimation of the cell-covered area in each image of the stack and (ii) calculation of a number of parameters (e.g., cell-covered area, cells' eccentricity, symmetry and intensity) that can be used for sample

characterisation. Once the images are collected, such parameters can be modified and an offline analysis can be performed on the same data set. Each algorithm provides specific advantages depending on the type of analysis and the sample properties, such as cell concentration and translucency.

Three main types of analysis can be performed: (i) segmentation, (ii) growth kinetics and (iii) cell proliferation and migration. The segmentation algorithm identifies and quantifies feature belonging to individual objects (or groups of objects) within the sample, such as microbes, spores and cells. The growth kinetics algorithms allow monitoring of microbial growth and growth inhibition over time. This also includes antimicrobial susceptibility testing (AST) and determination of minimum inhibitory concentration (MIC) value for antimicrobial compounds[24]. In this regard, the oCelloScope provides a semi-quantitative method, where positive controls should be always included in the analysis. This is also crucial in order to remove the influence of bacterial settling when performing growth analysis. Finally, the cell proliferation algorithm quantifies mammalian cell division and proliferation using the total area covered by cells. This finds application in monitoring mammalian cell migration and proliferation[25], as well as scratch wound healing assays.

These kinds of analysis, together with the oCelloScope technology have been shown to provide considerable advantages in several research fields, from microbiology[24] to medicinal chemistry[26] and pharmaceutical biotechnology,[27] as well as having great potential in basic cancer biology.[28] Furthermore, the different algorithms are implemented in a software program (UniExplorer) that provides a user-friendly interface for adjusting the experimental settings and achieving high-quality image data (Fig. 2). The output data can also be exported (e.g., to Microsoft Excel) for further processing. In addition, the software supports the automatic generation of time-lapse videos of the recorded images. The software communicates with the imaging system via an Ethernet connection, thereby allowing for design of the experiment, monitoring of cells and processing of data outside of the laboratory, which is a considerable advantage when working with microorganisms that require a high biosafety level.

Proven Applications and Future Developments

To date, the oCelloScope imaging system has found a large application area in monitoring bacterial and fungal growth (Fig. 3), growth kinetics and growth inhibition[26,29–31], as well as investigating dynamic changes in cell morphology over time[32,33] (Fig. 4). Fredborg et al. demonstrated that the system can be succesfully used for distinguishing between different growth patterns in filamentous bacteria[34] (Fig. 5) and detecting a statistically significant effect of antibiotics within only 6 minutes with a level of accuracy comparable to commercially available methods.[23,24] Within this same field of application, Uggerhøj et al. showed that the oCelloScope can be used to determine the MIC of antimicrobial peptides, even when the MIC could not be reliably evaluated with more conventional assays based on standard broth microdilution due to the formation of aggregates in solution.[26] Results such as these are particularly relevant since bioanalytical research constantly warrants advanced technologies able to perform faster and higher throughput analysis for monitoring microbial susceptibility to drugs and, in general, cellular responses to toxic agents (Fig. 6).

As the oCelloScope system facilitates the visualisation of low bacterial concentrations, it improves the ability to capture the important early stages in microbial growth that could not otherwise be detected with conventional optical density measurements.[23] This significantly reduces hands-on and incubation times when performing experiments and analyses, thus shortening the time required for obtaining results. Moreover, as the technology is based on an optical method, it has the advantage of focusing on the specific microorganism of interest, hence excluding any other type of cell in a mixed population or exogenous contaminants in a clinical or environmental isolate. Together, these advances and advantages highlight the great potential our technology offers for designing early targeted antibiotic therapy and for creating new perspectives that can lead to novel applications in the fields of mammalian cell research,[28] which may soon give further insights in the fields of cancer biology, personalised medicine, and stem cell research.

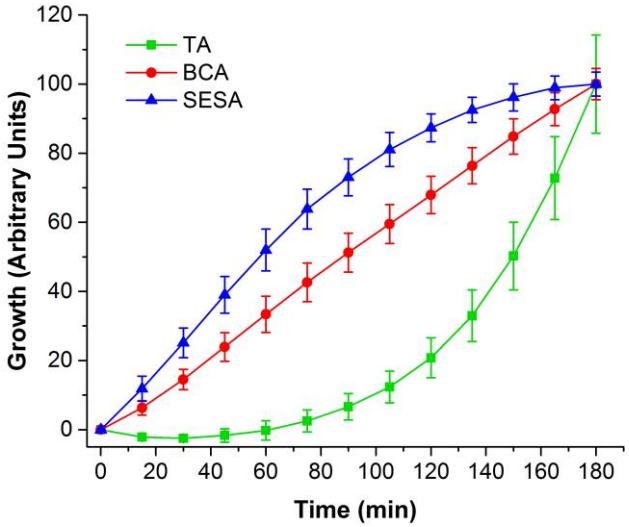

Figure 3. Monitoring of *Staphylococcus aureus* growth over time using the oCelloScope and the Background Corrected Absorption (BCA), Segmentation and Extraction of Surface Area (SESA) and Total Absorption (TA) algorithms (mean ± SD, n = 8). Each algorithm is designed to have specific advantages depending on the type of analysis and the sample properties. The BCA algorithm is based on the same principle of optical density (OD) measurements, but with increased sensitivity and robustness even at very low or high cell concentrations. The SESA algorithm identifies all the objects in a scan based on their contrast against the background and then calculates the total surface area covered by such objects. It is not sensitive to background intensity changes (caused by, e.g., condensation on the microtiter plate lid) and can measure microbial growth with high accuracy at very low cell concentrations. However, when more than 20% of the total image area is covered by objects, the SESA algorithm accuracy starts to decline. The TA algorithm is designed as an equivalent of OD measurements. TA sensitivity is limited if compared to the BCA algorithm, as growth and cell concentration need to be quite considerable before affecting light transmission. When monitoring bacterial growth over time, the starting cell concentration should be optimised depending on the type of microbes and the time of analysis. A starting concentration of 10^4 cells/mL is suggested when monitoring *Escherichia coli* growth in 96-well plates (100 µL/well) over 24 hours.

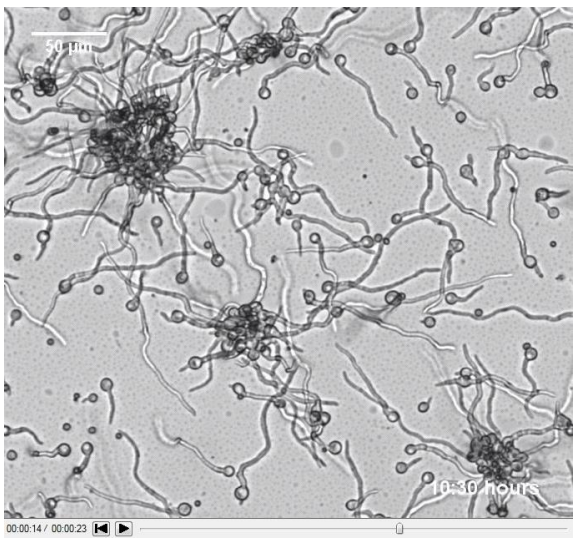

Figure 4. Video frame of a time-lapse video showing *Aspergillus niger* development over time. Images can be used for generation of growth curves as well as for quantification of changes in morphology using the SESA algorithm.

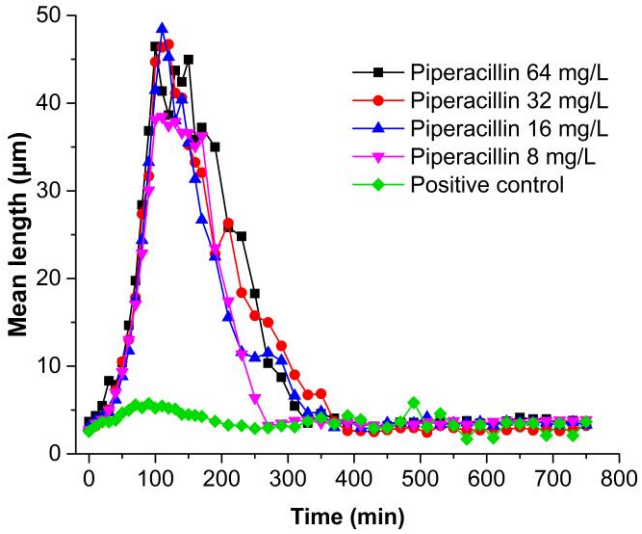

Figure 5. Effect of different concentrations of the β-lactam antimicrobial, piperacillin, on bacterial length of *Escherichia coli* from blood culture monitored using the oCelloScope imaging system and the Segmentation Extraction of Average Length (SEAL) algorithm. The SEAL algorithm allows discrimination between bacterial growth and filamentation. It also determines the average bacterial length along the major axis and performs segmentation.

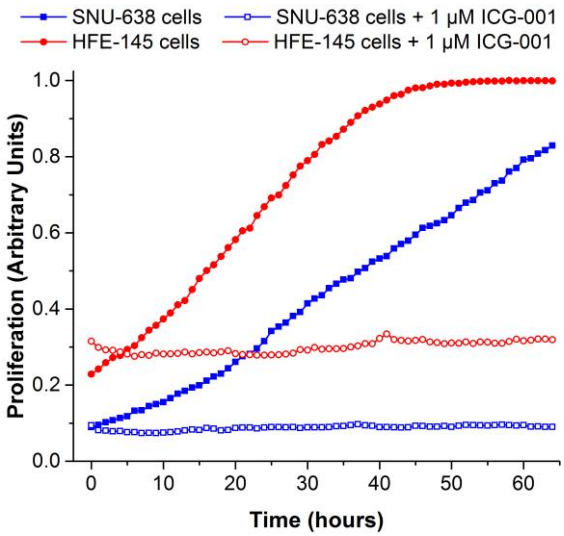

Figure 6. Response of two different gastric cell lines (SNU-638 and HFE-145) to ICG-001, a small molecule antagonist of β-catenin/T cell factor signaling. The deregulation of this biochemical pathway is of great interest as it is involved in most colon cancers. Studies were performed in collaboration with the Department of Clinical Biochemistry at Næstved Hospital (Næstved, Denmark).

References**

(1) Smart, R., and Spooner, D. F. (1972) Microbiological spoilage in pharmaceuticals and cosmetics. *J. Soc.Cosmet.Chem 23*, 721–737.
(2) Michelini, E., Simoni, P., Cevenini, L., Mezzanotte, L., and Roda, A. (2008) New trends in bioanalytical tools for the detection of genetically modified organisms: An update. *Anal. Bioanal. Chem. 392*, 355–367.
(3) Anderson, A. C. (2003) The process of structure-based drug design. *Chem. Biol. 10*, 787–797.
(4) Bailey, J. E. (1991) Toward a science of metabolic engineering. *Science (80-.). 252*, 1668–1675.
(5) Abraham, V. C., Taylor, D. L., and Haskins, J. R. (2004) High content screening applied to large-scale cell biology. *Trends Biotechnol. 22*, 15–22.
(6) Clatworthy, A. E., Pierson, E., and Hung, D. T. (2007) Targeting virulence: a new paradigm for antimicrobial therapy. *Nat. Chem. Biol. 3*, 541–548.
(7) Cho, S.-H., Jeon, J., and Kim, S. Il. (2012) Personalized medicine in breast cancer: A systematic review. *J. Breast Cancer 15*, 265.
(8) Taylor, D. L., Woo, E. S., and Giuliano, K. a. (2001) Real-time molecular and cellular analysis: the new frontier of drug discovery. *Curr. Opin. Biotechnol. 12*, 75–81.
(9) Ziauddin, J., and Sabatini, D. M. (2001) Microarrays of cells expressing defined cDNAs. *Nature 411*, 107–110.

(10) Stephens, D. J., and Allan, V. J. (2003) Light microscopy techniques for live cell imaging. *Science (80-.). 300*, 82–87.
(11) Pepperkok, R., and Ellenberg, J. (2006) High-throughput fluorescence microscopy for systems biology. *Nat. Rev. Mol. Cell Biol. 7*, 690–696.
(12) Selinummi, J., Ruusuvuori, P., Podolsky, I., Ozinsky, A., Gold, E., Yli-Harja, O., Aderem, A., and Shmulevich, I. (2009) Bright field microscopy as an alternative to whole cell fluorescence in automated analysis of macrophage images. *PLoS One 4*.
(13) Ettinger, A., and Wittmann, T. (2014) Fluorescence live cell imaging. *Methods Cell Biol. 123*, 77–94.
(14) Rieder, C. L., and Khodjakov, A. (2003) Mitosis through the microscope: advances in seeing inside live dividing cells. *Science (80-.). 300*, 91–6.
(15) Qiang, W., Merchant, F. A., and Castleman, K. R. (2008) Microscope image processing (Qiang, W., Merchant, F. A., and Castleman, K. R., Eds.) 1st Ed. Elsevier Inc., Burlington, MA, USA.
(16) Murphy, D. (2001) Fundamentals of light microscopy and electronic imaging. *Imaging* 1st Ed. John Wiley & Sons, Inc., Baltimore, MD, USA.
(17) Bozzola, J. J., Webster, P., Kuo, J., Ellis, E. A., Hendricks, G. M., Chandler, D. E., Sharp, W. P., Kaech, A., Ziegler, U., Grabenbauer, Ma., Han, H.-M., Huebinger, J., Chlanda, P., Sachse, M., Harris, J. R., de Carlo, S., Coughlin, M., Groen, A. C., Mitchison, T. J., and Webster, A. (2014) Electron microscopy. *Methods Mol. Biol.* (Kuo, J., Ed.) 3rd Ed. Humana Press, Hatfield, Hertfordshire, UK.
(18) Zernike, F. (1942) Phase contrast, a new method for the microscopic observation of transparent objects part II. *Physica 9*, 974–986.
(19) Price, R., and Gray, G. W. (2011) Basic confocal microscopy (Price, R., and Gray, G. W., Eds.). Springer.
(20) Frigault, M. M., Lacoste, J., Swift, J. L., and Brown, C. M. (2009) Live-cell microscopy - tips and tools. *J. Cell Sci. 122*, 753–767.
(21) Walter, R. J., and Berns, M. W. (1981) Computer-enhanced video microscopy: digitally processed microscope images can be produced in real time. *PNAS 78*, 6927–6931.
(22) Coutu, D. L., and Schroeder, T. (2013) Probing cellular processes by long-term live imaging - historic problems and current solutions. *J. Cell Sci. 126*, 3805–3815.
(23) Fredborg, M., Andersen, K. R., Jorgensen, E., Droce, A., Olesen, T., Jensen, B. B., Rosenvinge, F. S., and Sondergaard, T. E. (2013) Real-time optical antimicrobial susceptibility testing. J. Clin. Microbiol. 51, 2047–2053.
(24) Fredborg, M., Rosenvinge, F. S., Spillum, E., Kroghsbo, S., Wang, M., and Sondergaard, T. E. (2015) Rapid antimicrobial susceptibility testing of clinical isolates by digital time-lapse microscopy. Eur. J. Clin. Microbiol. Infect. Dis. 34, 2385–2394.
(25) Pijuan-Galitó, S., Tamm, C., Schuster, J., Sobol, M., Forsberg, L., Merry, C. L. R., Pijuan-galito, S., and Annerén, C. (2016) Human serum-derived protein removes the need for coating in defined human pluripotent stem cell culture. Nat. Commun 7, 1–12.
(26) Uggerhøj, L. E., Poulsen, T. J., Munk, J. K., Fredborg, M., Sondergaard, T. E., Frimodt-Moller, N., Hansen, P. R., and Wimmer, R. (2015) Rational design of alpha-helical antimicrobial peptides: Do's and don'ts. ChemBioChem 16, 242–253.
(27) Kjeldsen, T., Sommer, M., and Olsen, J. E. (2015) Extended spectrum β-lactamase-producing Escherichia coli forms filaments as an initial response to cefotaxime treatment. BMC Microbiol. 15, 1–6.
(28) Ashley, N., Jones, M., Ouaret, D., Wilding, J., and Bodmer, W. F. (2014) Rapidly derived colorectal cancer cultures recapitulate parental cancer characteristics and enable personalized therapeutic assays. J. Pathol. 234, 34–45.
(29) Aunsbjerg, S. D., Andersen, K. R., and Knøchel, S. (2015) Real-time monitoring of fungal inhibition and morphological changes. J. Microbiol. Methods 119, 196–202.
(30) Sørensen, J. L., Sondergaard, T. E., Covarelli, L., Fuertes, P. R., Hansen, F. T., Frandsen, R. J. N., Saei, W., Lukassen, M. B., Wimmer, R., Nielsen, K. F., Gardiner, D. M., and Giese, H. (2014) Identification of the biosynthetic gene clusters for the lipopeptides fusaristatin A and W493 B in Fusarium graminearum and F. pseudograminearum. J. Nat. Prod. 77, 2619–25.
(31) Wollenberg, R. D., Donau, S. S., Nielsen, T. T., Sørensen, J. L., Giese, H., Wimmer, R., and Søndergaard, T. E. (2016) Real-time imaging of the growth-inhibitory effect of JS399-19 on Fusarium. Pestic. Biochem. Physiol. 1–7.
(32) Khan, D. D., Lagerbä Ck, P., Cao, S., Lustig, U., Nielsen, E. I., Cars, O., Hughes, D., Andersson, D. I., and Friberg, L. E. (2015) A mechanism-based pharmacokinetic/pharmacodynamic model allows prediction of antibiotic killing from MIC values for WT and mutants. J. Antimicrob. Chemother. 70, 3051–3060.
(33) Jelsbak, L., Mortensen, M. I. B., Kilstrup, M., and Olsen, J. E. (2016) The in vitro redundant enzymes PurN and PurT are both essential for systemic infection of mice in Salmonella enterica serovar Typhimurium. Infect. Immun. 84, 2076–2085.
(34) Fredborg, M., Rosenvinge, F. S., Spillum, E., Kroghsbo, S., Wang, M., and Sondergaard, T. E. (2015) Automated image analysis for quantification of filamentous bacteria. BMC Microbiol. 15, 1–8.

[**]The articles reporting on the oCelloScope applications are highlighted in italic.